




A study of a biodegradable braided Mg stent for biliary reconstruction

Yue Zhang^{1,2}, Kaiyuan Chen^{1,2}, Huan Liu³, Yi Shao^{1,2,4}, Chenglin Chu^{1,2}, Feng Xue^{1,2}, and Jing Bai^{1,2,4,*} 

¹School of Materials Science and Engineering, Southeast University, Jiangning, Nanjing 211189, Jiangsu, China

²Jiangsu Key Laboratory for Advanced Metallic Materials, Jiangning, Nanjing 211189, Jiangsu, China

³College of Mechanics and Materials, Hohai University, Jiangning, Nanjing 211100, China

⁴Institute of Biomedical Devices (Suzhou), Southeast University, Suzhou 215163, Jiangsu, China

Received: 24 June 2020

Accepted: 21 August 2020

Published online:
15 September 2020

© Springer Science+Business
Media, LLC, part of Springer
Nature 2020

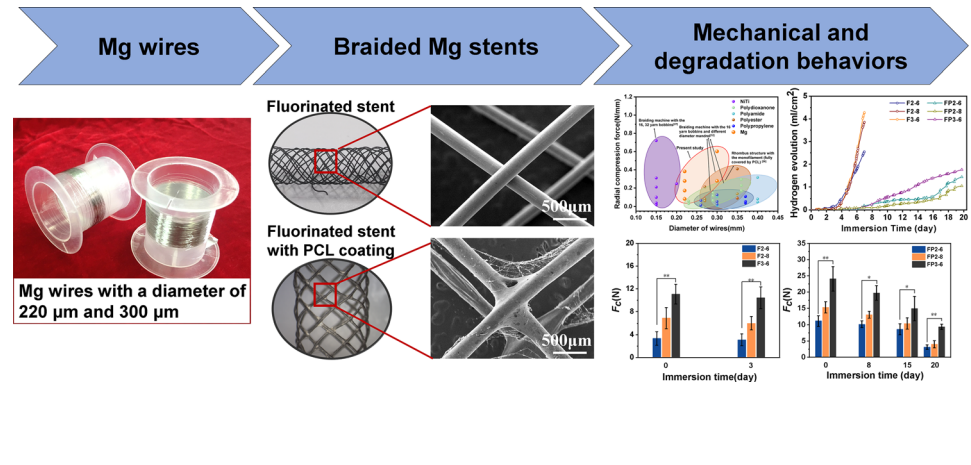
ABSTRACT

Aiming at deficiencies in non-degradable stents for benign common bile duct obstruction, the magnesium (Mg)-based braided stents were developed with one monofilament as a pilot research in this paper. We designed stents with the different monofilament diameter, braided-pin number and surface treatment systematically to study the mechanical and degradation behaviors. The results suggest the fluorinated Mg stents and them with polycaprolactone (PCL) coating can achieve the compression force of 3.35–11.07 N and 11.09–24.08 N, and even maintain 3.10–10.43 N for 3 days immersion and 3.11–9.37 N for 20 days immersion respectively. PCL coating on monofilament can provide significantly better compression force and corrosion resistance. By comparison with the stent in clinic, these Mg stents are expected to meet the demand of the radial compression force and implantation time. Furthermore, the degradation occurs at the ends preferentially for all stents, but for stents without PCL coating, the intersections of wire-mesh are also the area easily corroded. Additionally, the result of the compression test indicates the radial compression force is improved with the increase of monofilament diameter and pins number, but the recovery capability decreases slightly.

Handling Editor: Annela M. Seddon.

Address correspondence to E-mail: baijing@seu.edu.cn

GRAPHIC ABSTRACT



Abbreviations

CBD	Common bile duct
FDA	Food and Drug Administration
PCL	Polycaprolactone
F_c	Radial compression force
$E_{recovery}$	Elastic recovery ratio

Introduction

Common bile duct (CBD) obstruction is a common disease occurring in hepatobiliary surgery, causing the thorniest issue for patients and surgeons. Implanting T tube drainage made of silicone rubber has widely been used to support CBD after removing the CBD stone, but it still has many complications during treatment [1, 2]. With the development of interventional therapy and materials science, various biliary stents are prepared for biliary stricture to prevent stenosis and support the reconstruction. Common materials including nitinol alloy, stainless steel and plastic, are used for biliary stents to guarantee enough supporting force with good bending and compliance properties [3–5]. These stents have good clinical efficacy but needed to be reserved in the body or removed by secondary operation [3]. Recently, as the application of biodegradable materials in vascular stents and orthopedic implantation,

biodegradable biliary stents have emerged in bile duct therapy. Almeida et al. [6] investigated the reported data and found biodegradable versus multiple plastic stent implantation in benign biliary strictures reported lower complication rates, except for cholangitis and haemobilia.

To date, studies on biodegradable biliary stent mainly focused on polymer materials such as polylactic acid (PLA) [7, 8], poly(lactic-co-glycolic acid) (PLGA) [1], polydioxanone (PDO) [9], authorized by the FDA for clinical use. Gregory et al. [7] firstly evaluated the feasibility of PLA biliary stent in a porcine model, and the result showed the stent could remain patent up to 6 months, but the occlusion and migration remain concerns. Other disadvantages including long degradation time and insufficient strength also limit their application. Magnesium (Mg) is one of the most common metals in nature and also a constant element in the human body. In the past decades, Mg and its alloys have attracted continuously rising attention as biodegradable materials due to their good mechanical properties and biocompatibility [10]. The research of Mg alloys coronary stents has been the most popular field in medicine. The Mg coronary stents named Magmaris based on DREAMS 2 G from Biotronik Inc. obtained CE approval in June 2016 [11]. Different from vascular stents usually prepared by laser engraving, the braided technique has been applied for self-expandable metallic stents clinically during the development process of the non-vascular stent. It is still the most suitable technique,

owing to the produced structures exhibiting good mechanical strength, high shape recovery and flexibility [12]. Nevertheless, due to the limitation of high-performance Mg wire preparation, there have been no papers studied biodegradable Mg biliary stent fabricated by Mg monofilament. The feasibility of Mg alloys in the bile duct has been reported by several exploratory studies in recent years. Chen et al. [13] implanted Mg–6Zn alloy tubes in rabbits and mice for 7 days, and found the tube did not induce significant apoptosis. Moreover, their further research demonstrated these tubes were obviously degraded after 1 week and remained only 9% after 3 weeks of implantation [14]. Liu et al. [11] also evaluated the response of AZ31 alloy tube as biliary stents in rabbits for 6 months, and the result from histology and whole blood analysis confirmed the biosafety. These findings displayed the prospect of application of Mg alloys in biliary implantation, but they all used Mg tubes which is far from the actual stent, especially resulting in the incapable study on the changes of mechanical properties of braided Mg biliary stent during degradation which is an important data for evaluating service performance.

Recently, Mg–Zn–Ca series alloys have attracted extensive attention as biodegradable materials [15]. Both Zn and Ca are essential elements in the human body and are biocompatible within certain limits [16]. These alloying elements are also effective grain refiners for magnesium and expected to improve the strength and ductility [17, 18]. Therefore, ZX20 alloy monofilament was used in this paper. A series of biodegradable Mg biliary stents with the rhombic mesh structure were fabricated with different monofilament diameter, braid-pin number and surface treatment. The effect of the structure of Mg stents on the supporting capacity was evaluated by the compression test. On the other hand, the high degradation rate of Mg alloys in vivo and in vitro is the main reason hindering their application in the medical field. For biodegradable materials, the mechanical properties of implants will be changed during the degradation process, which eventually influences the treatment effect. Therefore, the degradation behavior and the changes of the compression force in the process of degradation of various stents were also investigated.

Materials and methods

Materials

ZX20 (wt%: Zn 2.281; Ca 0.311; Al 0.032; Si 0.0319; Mn 0.0255; Ni 0.0026; Fe 0.0021; Cu 0.005; Mg remaining) wires (Fig. 1a), developed by our research group [19–21] and produced by Suzhou Jingjun New Materials Technology Co., Ltd. China, with a diameter of 0.22 mm and 0.30 mm were used in this study. Their representative tensile engineering stress–strain curves depicted in Fig. 1b with the mechanical property bar graph inserted. Among Mg alloys, both wires show very good ultimate strength and elongation with about 290 MPa and 16% for 0.22 mm wire and 300 MPa and 22% for 0.30 mm wire.

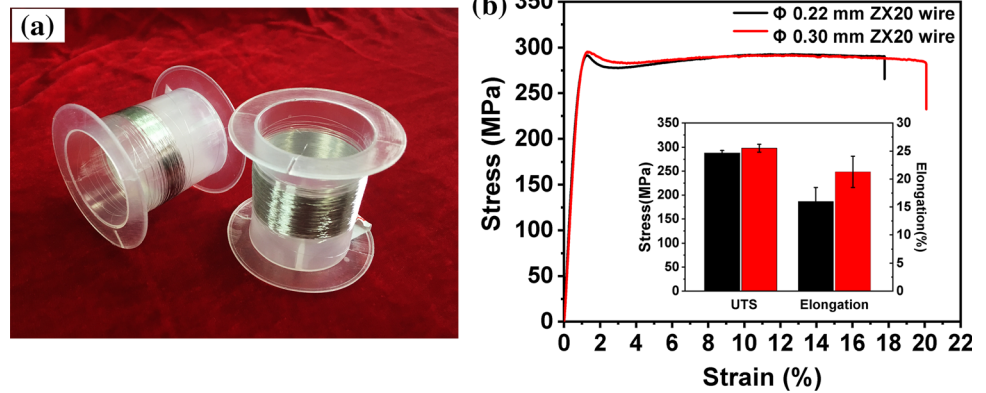
To improve the corrosion resistance of Mg stents, the fluoride treatment and polymer coating are also used on the surface of wires. The number average molecular weight of medical grade polycaprolactone (PCL) was $8.0 \times 10^4 \text{ g mol}^{-1}$. The hydrofluoric acid solution (40%) for fluorinated treatment, dichloromethane for dissolving PCL, and other chemicals such as cholesterol, sodium taurocholate from bovine bile, soybean lecithin were purchased from Sino-pharm Chemical Reagent Co., Ltd. China.

Methods

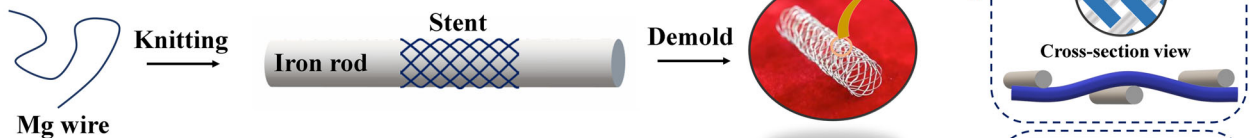
Preparation methods

In this study, we fabricated two types of biodegradable Mg biliary stent through fluorinated treatment and fluorinated treatment then coated with PCL film for better protection of the Mg substrate. The preparation process of various braided Mg stents is illustrated in Fig. 2. The untreated stent was firstly knitted with ZX20 monofilament using a self-made cylinder of iron rod mold with a diameter of 8 mm, effective working lengths of 40 mm. The schematic diagram of structure was shown in Fig. 2a. After finishing the braiding process, the stent was washed in acetone by ultrasonic cleaner for 3–5 min and rinsed with deionized water for 1 min. Afterwards, it was immersed in an alkaline solution containing NaOH of 18 g L^{-1} , Na_2CO_3 of 46 g L^{-1} and Na_3PO_4 of 28 g L^{-1} for 2 min at $80 \text{ }^\circ\text{C}$. Immediately after the preprocessing procedure, the stent was immersed into hydrofluoric acid solution (40%) at room temperature for 48 h, and rinsed with deionized water,

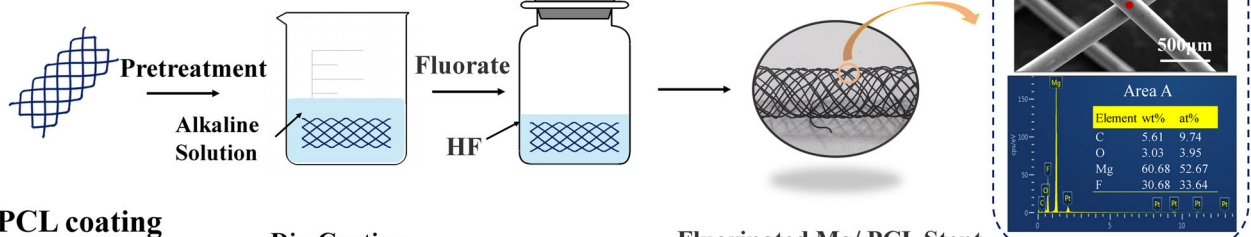
Figure 1 **a** The photograph of ZX20 wires, and **b** stress–strain curves of ZX20 wires with a diameter of 0.22 mm and 0.30 mm.



(a) Braiding process



(b) Fluorinated treatment



(c) PCL coating

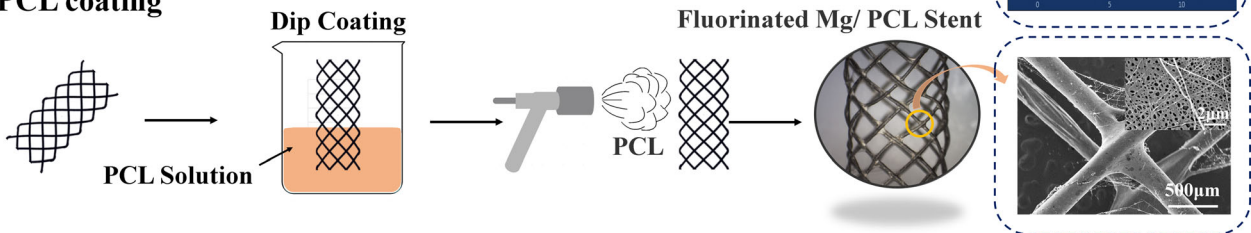


Figure 2 Illustration the preparation process of braided Mg biliary stents, **a** the braiding process of the bare stent with a rhombus structure, **b** the method of fluorinated treatment and the EDS

analysis on the surface, **c** the preparation of PCL coating on the fluorinated stent and the morphology of wire-mesh intersection and its surface.

ethanol and dried in drying oven at 37 °C for 30 min (Fig. 2b). For the stent with duplex coating, PCL was weighed and dissolved in dichloromethane to obtain 5% (w/v) solution, the fluorinated treated stent was dipped into the prepared solution for 2 min and then withdrawn with a speed of 2 cm s⁻¹ (Fig. 2c). After dip coating and drying in air, the sample was sprayed with 3% (w/v) PCL solution by pneumatic paint gun for 5–10 s under the pressure of 800 kPa. It is ensured that the thickness of PCL layer did not

exceed 30 μm. Specifications of each Mg biliary stents were shown in Table 1.

Cover factor defined as the percentage of mandrel surface covered by monofilaments is a good indicator of braided structure uniformity, it was calculated as follows.

$$\text{Cover factor} = 1 - \left(1 - \frac{WN}{4\pi R \cos \alpha} \right) \quad (1)$$

Table 1 Specifications of braided Mg biliary stents

Surface treatment	Samples code	Diameter of wire (mm)	Braiding number (pins)
Fluorination	F2-6	0.22	6
	F2-8	0.22	8
	F3-6	0.30	6
Fluorination + PCL coating	FP2-6	0.22	6
	FP2-8	0.22	8
	FP3-6	0.30	6

where W is the monofilament width (mm), N is the number of bobbins which is the double number of pins, R is the mandrel radius (mm), α is the braiding angle (rad).

Immersion test

In human bile, water constitutes approximately 85% of the volume of bile [22]. The major organic solutes in bile are bilirubin, bile salt, lecithin, and cholesterol, and the quaternary system of bile salt (or sodium taurocholate) -lecithin-cholesterol-water has long been used to study the in vitro formation of cholesterol gallstones [23]. In addition, inorganic ions such as Cl^- , Na^+ also participate to maintain osmotic pressure balance. Therefore, the simulated bile was prepared based on the Small's model system to be used for the immersion test to evaluate the changes of the compression force during degradation [24]. The simulated bile consisted of 30.47 mM sodium taurocholate, 16.62 mM lecithin and 2.77 mM cholesterol in 154 mM NaCl solution containing 50 mM Tris(hydroxymethyl)aminomethane. The pH of the solution was adjusted to 7.65. All immersion containers were kept at 37.5 ± 0.5 °C in the water bath. The ratio of the solution volume to the specimen area was 20 mL cm^{-2} according to ASTM G31-72 standard. Immersion solution was refreshed every 10 days. Samples were removed from the solution at a certain time, gently rinsed with distilled water and dried in air for observation. The corrosion products were removed with boiling chromic acid solution containing 10% CrO_3 .

Measurement of radial compression

The radial parallel plate compression test was commonly conducted to evaluate the compression characteristics of stents, and it was also adopted in this study on biliary stents at different degradation time

by a CMT4503 electronic universal testing machine. The illustration of radial compression test for stents was shown in Fig. S1 of the Supplementary. Specimens were pressed to deformation within 50% of the initial internal diameter of the biliary stent with the top platen loaded speed of 20 mm min^{-1} at room temperature. When the displacement of load platen reached 50% of the initial biliary stent diameter, the top compression platen was stopped, and the force value at the moment was defined as the radial compression force (F_c). After staying for 5 s, the compression platen was back to the original position with a speed of 20 mm min^{-1} . In the process of testing, the compression initial height was defined as the position when compression platen just contacted the biliary stent, and the stent was placed at the center of the bottom plate. The elastic recovery (E_{recovery}) facility of stent was evaluated by measuring the change rate of internal diameter according to the following equations.

$$E_{\text{recovery}} = \frac{D_2 - D_1}{D_0 - D_1} \quad (2)$$

where D_0 was the initial internal diameter of the stent before compression test, D_1 was the internal diameter of stent compressed to stop, D_2 was the internal diameter recovered after compression.

Morphology characterization

The macroscopic morphology of stents was observed by ZOOM 645S camera stereoscopic microscopy. Details of stents were examined by Sirion200 Field Emission Scanning Electron Microscope (FE-SEM, FEI, USA). The chemical composition in the micro area was detected by Aztec x-Max 80 energy dispersive spectroscopy (EDS, Oxford, UK).

Statistical analysis

Experimental data were presented as mean \pm standard deviation of three measurements. Statistical analysis was performed with SPSS 17.0 software (SPSS Inc., Chicago, USA). One-way analysis of variance (ANOVA) followed by the least significance difference (LSD) post-hoc test was used to statistical analysis among groups. A p value < 0.05 was considered a statistically significant difference.

Results

Characterization of stents

Braided Mg biliary stents fabricated with 8 pins and monofilament diameter of 0.22 mm after removing the iron rod model is shown in Fig. 2a. The original tubular structure is maintained stably without collapsing and constriction, and the local deformation of Mg wire is seen at intersecting positions. Figure 2b depicts characters of the stent after fluorinated treatment, and its surface after fluorinated treatment is smooth and contains much fluorine element, indicating the formation of the conversion coating. By comparison to the area of the wire-mesh intersection, there is a significant aggregation of PCL after dip coating and spraying with a PCL solution. Despite the presence of small and thin polymer net due to the solution rapidly cooling after injection, the mechanical properties of the stent are not enough to be affected by them. Like previous studies, a porous PCL film is also prepared on the surface (Fig. 2c).

Compression performance of stents

Figure 3a shows the cover factor of stents with different structures, in comparison to pins number, the monofilament diameter has a stronger influence on it. The compression curves of stents were plotted as depicted in Fig. 3b. It is apparent that an obvious compression platform of fluorinated stents exists when the compression ratio of D_0 is about 30%, indicating the stents have reached their supporting limitations, whereas no platforms are observed on stents coated by PCL. The stents coated with PCL have higher compression force than that of their corresponding fluorinated stents. Furthermore, the radial compression force and recovery ratio of stents

diameter obtained from the compression curve are summarized in Fig. 3c, d. In terms of stents without PCL coating, F_c of the stent with 6 pins and wire diameter of 0.22 mm is about 3.35 N. As the pin number increase to 8, F_c increases slightly to about 6.88 N. Simultaneously, increasing the diameter of wire has a similar trend and F_c of F3-6 is about 3.3 times that of the F2-6, which is more significant and effective. However, as the F_c increases, the decrease of E_{recovery} is also observed in Fig. 3d. The reduction of the recovery rate by increasing the diameter of the wire is more obvious than that by the increasing of pins number. Besides, a similar phenomenon is observed on the coated stents.

Degradation behaviors

Hydrogen evolution tests

To further evaluate the corrosion resistance of samples for a long term, evolved hydrogen volumes were measured as a function of immersion time until 7 days and 20 days for stents without and with PCL coating respectively, as depicted in Fig. 4. At the initial stage of immersion, a small amount of bubbles is collected from the surface of fluorinated Mg stents and no bubbles are observed on the surface of the sample with PCL coating, suggesting there is an effective corrosion protection of both two surface treatment methods. Nevertheless, the hydrogen volume of fluorinated samples begins to increase rapidly at an immersion of 4 days. As a comparison, the hydrogen volume of stents with PCL coating begins to slightly rise after 6 days of immersion and finally becomes rapidly higher after 13–15 days of immersion.

Degradation morphologies

The obtained macroscopic feature of fluorinated Mg stents with and without PCL coating after immersion in simulated bile is shown in Fig. 5. For the fluorinated stent, the overall structure of Mg stents remains almost intact after 3 days' immersion while they are seriously corroded after immersion for 6 days. The structure of the F3-6 stent is even disintegrated as a binding force between wires disappearing. In the case of stents with PCL coating, the skeleton of the stents is not broken after 8 days' immersion. As the soaking time increases, it can be seen that some areas have

Figure 3 **a** The cover factor and **b** representative compression curves of various Mg stents, **c** data statistics with compression force at 50% of D_0 and **d** the diameter recovery ratio after compression test ($*p < 0.05$; $**p < 0.01$).

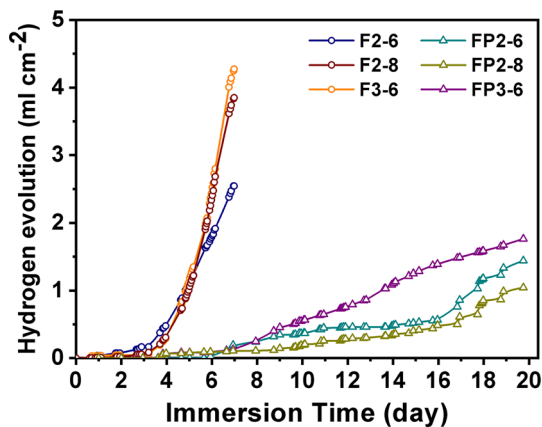
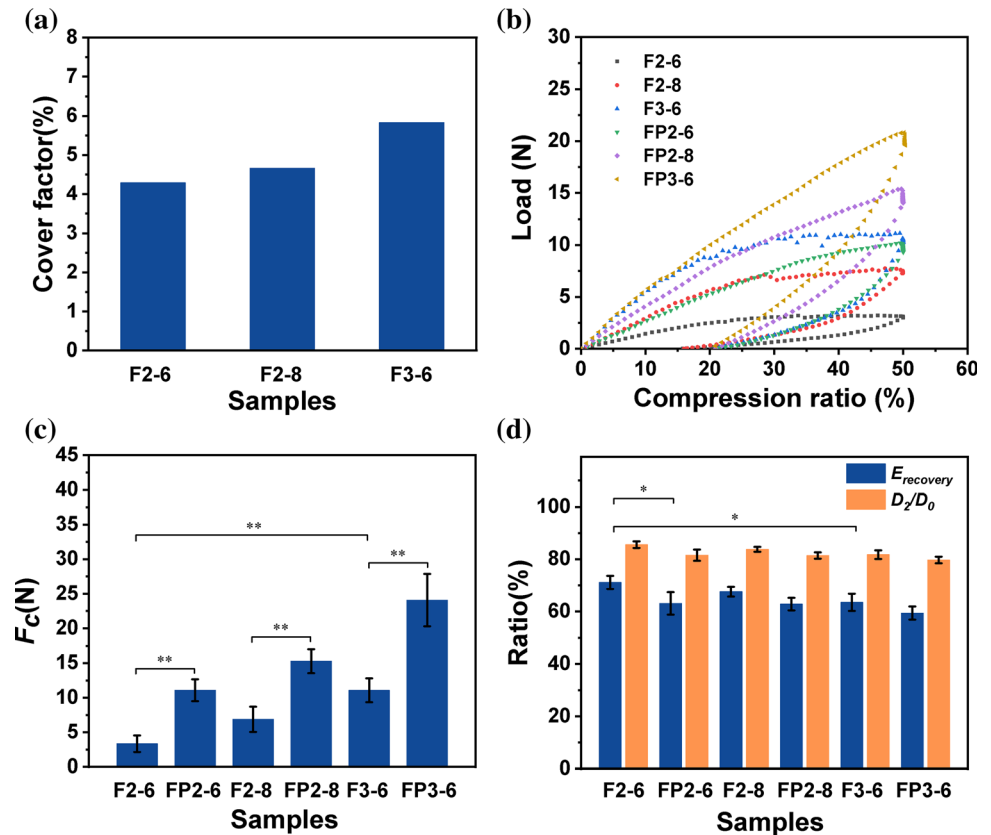


Figure 4 The dependence of hydrogen evolution on immersion time in simulated bile at 37 °C for different experimental samples.

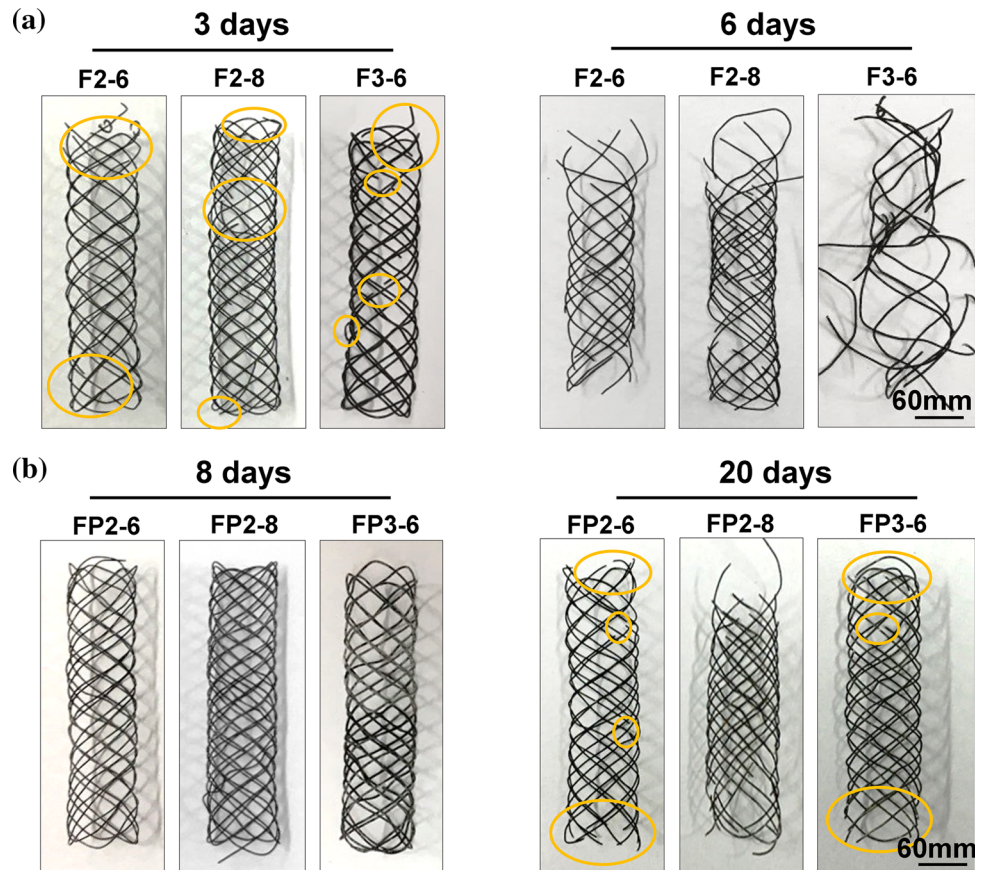
been damaged. In addition, Fig. 6 depicts the SEM images of representative corroded position. As shown in Fig. 6a, d, there are obvious cracking sites subjected to the stress corrosion. As the braid-pin number and diameter of wire increase, the broken positions begin to be distributed randomly due to more stress in the supporting structure of stents. Typical morphologies of corrosion fracture under stresses on both sides are seen in Fig. 6b, c, e. Besides,

the obvious corrosion at the wire-mesh intersection is also observed in Fig. 6f, which might be due to inadequate fluorination at the contact area. For the stent with PCL coating, little small corrosion pits are observed after 8 days, indicating the solution has penetrated the PCL coating and begins to corrode fluorinated conversion film. Furthermore, dense corrosion pits are observed after 15 days as shown in Fig. S2 of Supplementary files, suggesting the expansion of corrosion pits and the increase of damage positions. And then, the corrosion becomes more severe with increasing immersion time especially on the latter days of immersion, in accordance with the results of the hydrogen evolution experiment. There are many significant breakages of stents and more obvious damages at both ends.

Evolution of the compression performance

Figure 7 shows the F_c and $E_{recovery}$ changes of these Mg stents versus immersion time. It can be found that F_c of all fluorinated Mg stents decreases only a little even after 3 days' immersion because the main structure of stents remains intact (Fig. 7a). For the

Figure 5 The photographs of **a** experimental fluorinated Mg stents after 3 and 6 days' immersion, and **b** fluorinated Mg stents with PCL coating after 8 and 20 days' immersion.



braid-pin number of 6, E_{recovery} remains basically the same as that of primary samples, but the E_{recovery} of FP2-8 decreases significantly and is about 59.55% (Fig. 7b). These changes may be attributed to the broken position at intersections of wire-mesh and the fracture of a localized corrosion pit under compression stress. On the other hand, for the stent with PCL coating, it is obvious that the F_c decreases gradually versus immersion time as shown in Fig. 7c. The rapid decrease occurs after 15 days' immersion, which is consistent with changes in hydrogen evolution tests.

Discussion

Advantages of braided Mg stents for biliary reconstruction

Different biliary stents associated with the alteration of materials and structures have been reported in the literature for obtaining optimal stent design [25]. The radial compression force is of importance for maintaining the structure of the biliary tract. Figure 8

shows the radial compression force in unit length of the several braided fibrous stents including nitinol and diverse polymers stents [12, 26, 27]. It is noted that the compression force of commercial MTN-DA biliary stent (produced by Micro-Tech Co., Ltd. China) fully covered with PCL is about 0.14 N mm^{-1} , and that of nitinol stents braided by machine with a diameter of 0.15 is $0.02\text{--}0.72 \text{ N mm}^{-1}$. The stents fabricated with polyamide and polyester demonstrate good compression properties, but they are hard to degrade in the body. Additionally, PDO is another biodegradable material with promising applications in recent years. The stents braided with PDO monofilament then fully covered with PCL also have enough radial compression force, but overmuch PCL takes too long to degrade completely. The strength of Mg alloys has long been controversial especially in the process of degradation. However, comparing to these reported studies, it could be noticed that the studied Mg stent has a relatively high compression force though the diameter of wire is smaller than polymers, which is beneficial to the endothelialization of the stent to improve the success rate of

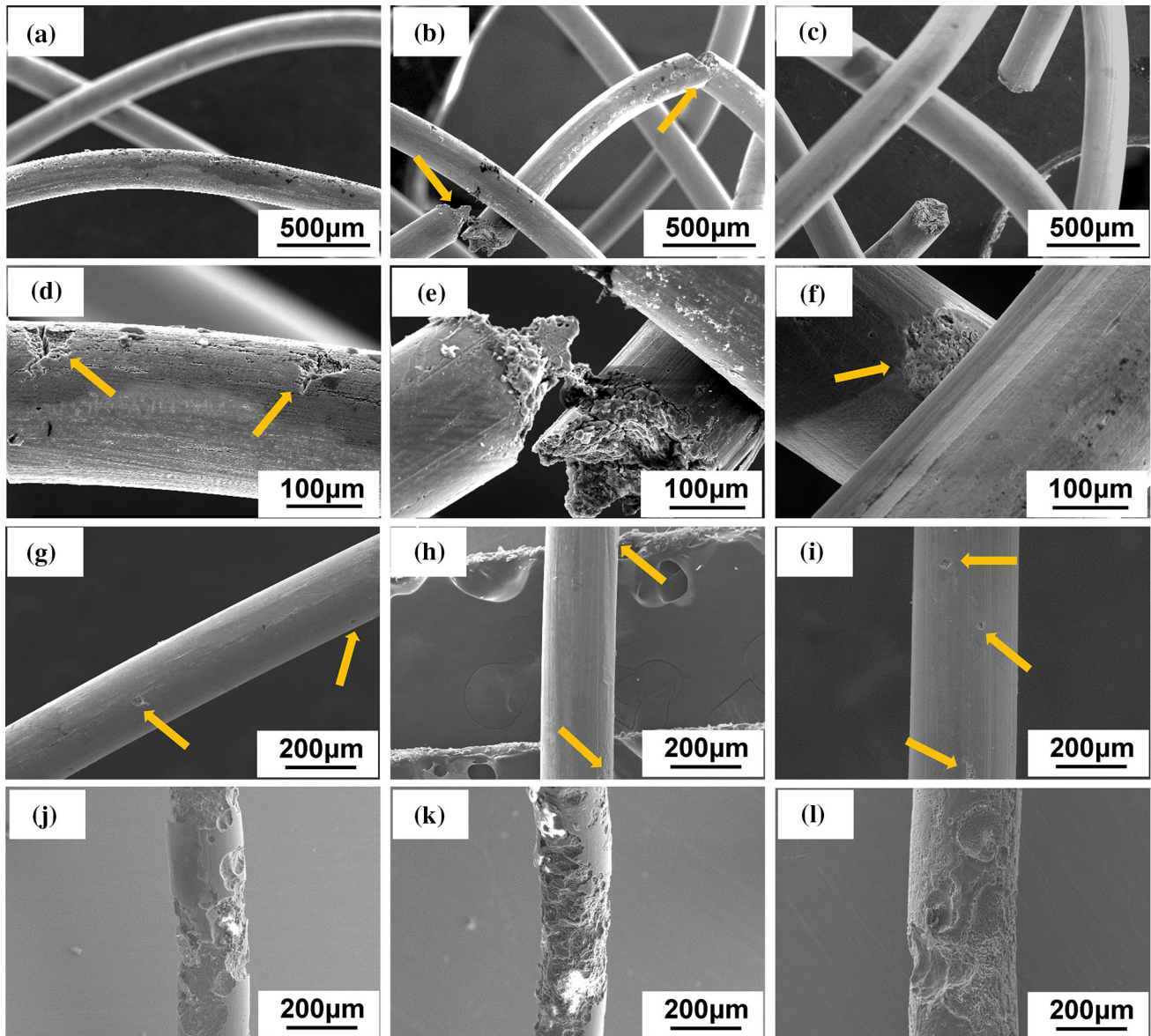


Figure 6 The representative morphologies of fluorinated Mg stents immersed for 3 days after removal of corrosion products, low magnification: **a** F2-6, **b** F2-8, **c** F3-6; high magnification: **d** F2-6, **e** F2-8, **f** F3-6, and morphologies of wires from fluorinated

stents with PCL coating immersed for 8 days: **g** FP2-6, **h** FP2-8, **i** FP3-6; and 20 days: **j** FP2-6, **k** FP2-8, **l** FP3-6, after removal of the PCL and corrosion products.

implantation [28]. Moreover, the fluorinated Mg stents and them with PCL coating can maintain $0.08\text{--}0.26\text{ N mm}^{-1}$ for 3 days immersion and $0.08\text{--}0.23\text{ N mm}^{-1}$ for 20 days immersion respectively. On the other hand, for the benign CBD construction, an ideal biliary stent should disappear automatically after healing. Previous studies of biodegradable Mg alloys have reported they did not perform well because of their rapid degradation, especially in the position with mechanical action and

fluid environment for long time healing [10]. Nevertheless, in the field of bile duct surgery, the support time required after CBD surgery is approximately 7 to 10 days, and the non-degradable stent generally needed removed 1 week later [14]. Moreover, the complicated CBD circumstances may contribute to a lower degradation rate in the body [29]. The surface of the stent is often covered with sediment and bile duct endothelial cells, acting as a barrier to retard further corrosion [30]. Therefore, these Mg stents are

Figure 7 F_c and $E_{recovery}$ changes of several Mg stents versus immersion time for stent without PCL coating (a, b), and for stents with PCL coating (c, d) ($*p < 0.05$; $**p < 0.01$).

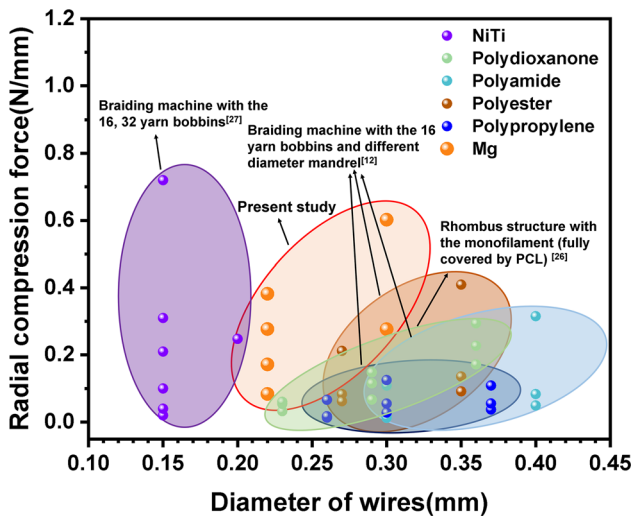
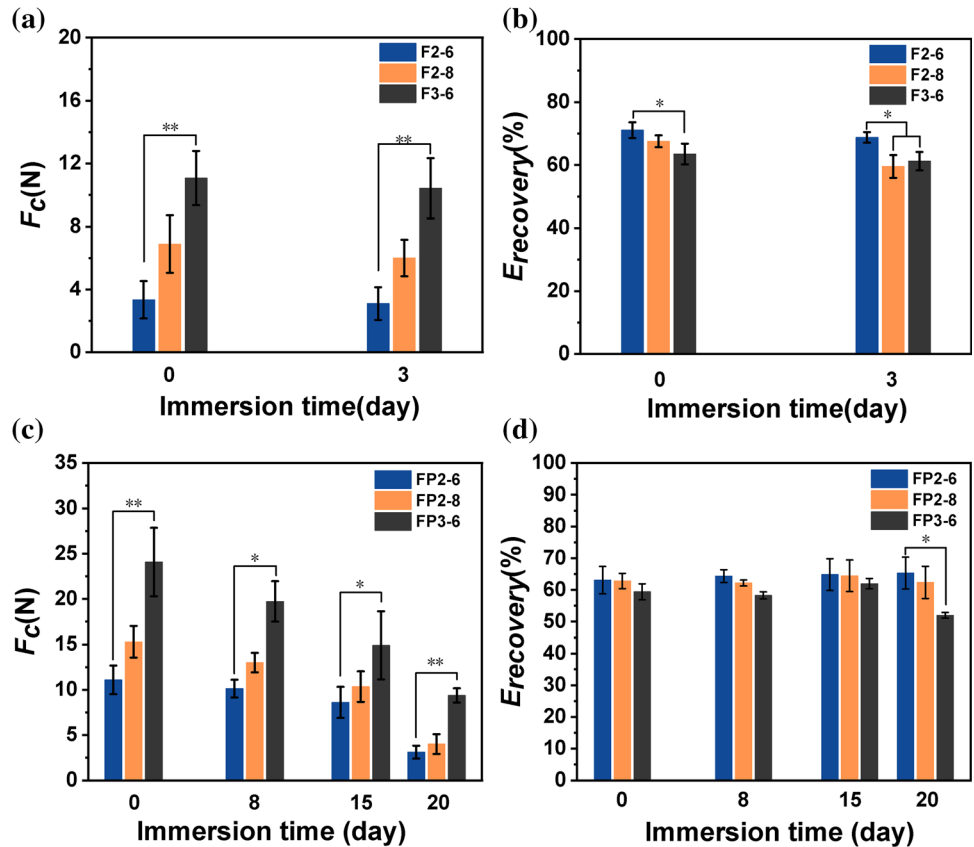


Figure 8 The comparison of the radial compression force in unit length of several braided fibrous stents.

expected to meet the radial force and supporting time.

Influence of diameter, pins number and PCL coating on compression performance

In general, the properties of braided stents are highly dependent on structural factors such as the diameter of monofilament, bobbins number and coating. Based on the iron mold we designed, the stent with 8 pins provides a total of 128 wire-mesh intersections, which is more than 72 intersections of 6 pins stents. Therefore, for the same diameter of monofilament, with the increase of brain-pin number, the structural unit of the stent becomes smaller, leading the limitations of mesh deformation and increases the force bearing points. Similarly, as the same braid-pin number of stents, the growth of monofilament diameter increases the resistance of bending and buckling under the compression. Furthermore, it is noted that the increase of the wire diameter is more significant and effective to improve the compression force than the increase of pins number, which is due to the increase of diameter not only increases the cover factor but also increases the thickness of stents. In terms of stents with PCL coating, the aggregation of PCL at intersections of wire-mesh as shown in Fig. 2c limits

the relative slip and bending deformation of interlacing points [31]. With the increase of the compression force, the recovery capacity of all stents decreases slightly, which is attributed to the plastic deformation of mesh-wire. Although the stent diameter could not recover completely back to the original value, the diameter recovery is more than 80% of initial internal diameter except the FP3-6 stent, which is comparable with the value obtained with previously reported polyamide and polypropylene stents [12].

Degradation behaviors of stents

Based on the evolution of morphologies and compression properties of stents during degradation, there are somewhat differences from that of wires in static immersion. Firstly, there is a large deformation at both ends of the stent because of the winding of wire in the knitting process, causing an amount of residual stress. Secondly, the wire between three interlacing points making up the braided structure is subjected to a force similar to the three-point bending, as shown in Fig. 2a. And thirdly, for stents without PCL coating, the local corrosion at intersections is not negligible. Yan et al. [32] evaluated the extruded AZ31B plate with fluorinated treatment in SBF, and demonstrated that no deposition could be found on the surface of the sample until to the 7 days. Therefore, under the influence of the above factors, fluorinated Mg stents can remain almost complete structure for 3 days' immersion, while the radial compression force has a little decline. As the corrosion progressing, the chemical transformation layer is gradually destroyed and the stent is disintegrated as the binding force between wires disappearing. Regarding stents with PCL coating, besides the structural factors, the role of PCL film hindering the interaction of the substrate with the solution is also the main factor for the degradation of stents. Cai et al. [20] evaluated the effect of surface modification on interfacial bonding by single wire pull-out experiments and found a higher bonding force leads to higher bending strength in wires/PLA composites. It is also reported the bonding force between PCL and MgF_2 is better than that between PCL and Mg substrate [33]. Thus, the degradation of stents with PCL coating is divided into two stages. First, the aqueous solution penetrates the PCL coating into the interface and begins to react with MgF_2 coating and substrate,

resulting in the decrease of interface adhesion and appearance of slight pitting, which is consistent with the increase of the hydrogen evolution result and the decline of properties in the first 15 days. And then, when the generation rate of hydrogen is more than the volume loss of substrate, the PCL coating will be broken under the internal stress, causing the increase of degradation rate [34, 35]. The radial compression force is obviously decreased from 15 to 20 days.

Overall, we conducted a primary exploration on Mg biliary stent braided with a monofilament, and presented the stents with good compression force and corrosion resistance. These biodegradable Mg stents might provide better options for healing benign CBD obstruction, and the corresponding work would be proceeded in further.

Conclusion

In this study, biodegradable Mg-based stents with and without PCL coating are successfully prepared by one magnesium monofilament for benign CBD obstruction. By comparing the compression force between other stents reported in literature, these stents can meet the clinical requirements of radial compression force, especially during the degradation process. Additionally, the compression force increases with the increase of monofilament diameter and braided-pin number, but the recovery capability decreased slightly. Based on the evolution of stents macroscopic morphologies versus immersion time, the degradation occurred at the ends stents preferentially for all stents, but for stents without PCL coating, the intersections of wire-mesh were also the area easily corroded. This work could provide a scientific basis for the fabrication of this kind of Mg stent to gain appropriate degradation time and support.

Acknowledgements

This work was supported by the National Key Research and Development Program of China (2016YFC1102402), the National Natural Science Foundation of China (51971062) and the Science and Technology Project of Jiangsu Province (BE2019679).

Electronic supplementary material: The online version of this article (<https://doi.org/10.1007/s10853-020-05289-9>) contains supplementary material, which is available to authorized users.

References

- [1] Xu XY, Liu TJ, Liu SH, Zhang K, Shen Z, Li YX, Jing XB (2009) Feasibility of biodegradable PLGA common bile duct stents: an in vitro and in vivo study. *J Mater Sci Mater Med* 20:1167–1173. <https://doi.org/10.1007/s10856-008-3672-2>
- [2] Daldoul S, Moussi A, Zaouche A (2012) T-tube drainage of the common bile duct choleperitoneum: etiology and management. *J Visc Surg* 149:e172–e178. <https://doi.org/10.1016/j.jvisurg.2012.03.008>
- [3] van Boeckel PG, Vleggaar FP, Siersema PD (2009) Plastic or metal stents for benign extrahepatic biliary strictures: a systematic review. *BMC Gastroenterol* 9:96. <https://doi.org/10.1186/1471-230X-9-96>
- [4] Elwir S, Sharzehi K, Veith J, Moyer MT, Dye C, McGarrity T, Mathew A (2013) Biliary stenting in patients with malignant biliary obstruction: comparison of double layer, plastic and metal stents. *Dig Dis Sci* 58:2088–2092. <https://doi.org/10.1007/s10620-013-2607-z>
- [5] Luigiano C, Ferrara F, Cennamo V, Fabbri C, Bassi M, Ghersi S et al (2012) A comparison of uncovered metal stents for the palliation of patients with malignant biliary obstruction: nitinol vs. stainless steel. *Dig Liver Dis* 44:128–133. <https://doi.org/10.1016/j.dld.2011.08.015>
- [6] Almeida GG, Donato P (2020) Biodegradable versus multiple plastic stent implantation in benign biliary strictures: a systematic review and meta-analysis. *Eur J Radiol* 125:108899. <https://doi.org/10.1016/j.ejrad.2020.108899>
- [7] Ginsberg G, Cope C, Shah J, Martin T, Carty A, Habecker P et al (2003) In vivo evaluation of a new bioabsorbable self-expanding biliary stent. *Gastrointest Endosc* 58:777–784. [https://doi.org/10.1016/S0016-5107\(03\)02016-9](https://doi.org/10.1016/S0016-5107(03)02016-9)
- [8] Girard E, Chagnon G, Broisat A, Dejean S, Soubies A, Gil H et al (2020) From in vitro evaluation to human postmortem pre-validation of a radiopaque and resorbable internal biliary stent for liver transplantation applications. *Acta Biomater* 106:70–81. <https://doi.org/10.1016/j.actbio.2020.01.043>
- [9] Mauri G, Michelozzi C, Melchiorre F, Poretti D, Tramarin M, Pedicini V et al (2013) Biodegradable biliary stent implantation in the treatment of benign bilioplastic-refractory biliary strictures: preliminary experience. *Eur Radiol* 23:3304–3310. <https://doi.org/10.1007/s00330-013-2947-2>
- [10] Zheng YF, Gu XN, Witte F (2014) Biodegradable metals. *Mater Sci Eng Res* 77:1–34. <https://doi.org/10.1016/j.mser.2014.01.001>
- [11] Liu Y, Zheng SM, Li N, Guo HH, Zheng YF, Peng JR (2017) In vivo response of AZ31 alloy as biliary stents: a 6 months evaluation in rabbits. *Sci Rep* 7:40184. <https://doi.org/10.1038/srep40184>
- [12] Rebelo R, Vila N, Figueiro R, Carvalho S, Rana S (2015) Influence of design parameters on the mechanical behavior and porosity of braided fibrous stents. *Mater Des* 86:237–247. <https://doi.org/10.1016/j.matdes.2015.07.051>
- [13] Chen YG, Yan J, Wang XH, Yu S, Wang ZG, Zhang XN et al (2014) In vivo and in vitro evaluation of effects of Mg–6Zn alloy on apoptosis of common bile duct epithelial cell. *Biomaterials* 27:1217–1230. <https://doi.org/10.1007/s10534-014-9784-x>
- [14] Chen YG, Yan J, Wang ZG, Yu S, Wang XH, Yuan ZM et al (2014) In vitro and in vivo corrosion measurements of Mg–6Zn alloys in the bile. *J Mater Sci Mater Med* 42:116–123. <https://doi.org/10.1016/j.jmsec.2014.05.014>
- [15] Ding PF, Liu YC, He XH, Liu DB, Chen MF (2019) In vitro and in vivo biocompatibility of Mg–Zn–Ca alloy operative clip. *Bioact Mater* 4:236–244. <https://doi.org/10.1016/j.bioactmat.2019.07.002>
- [16] Gu XN, Zheng YF, Cheng Y, Zhong SP, Xi TF (2009) In vitro corrosion and biocompatibility of binary magnesium alloys. *Biomaterials* 30:484–498. <https://doi.org/10.1016/j.biomaterials.2008.10.021>
- [17] Min Y, Debao L, Runfang Z, Minfang C (2018) Microstructure and properties of Mg–3Zn–0.2Ca alloy for biomedical application. *Rare Met Mater Eng* 47:0093–0098. [https://doi.org/10.1016/S1875-5372\(18\)30078-X](https://doi.org/10.1016/S1875-5372(18)30078-X)
- [18] Liu H, Sun C, Wang C, Li YH, Bai J, Xue F et al (2020) Improving toughness of a Mg–Ca-containing Mg–Al–Ca–Mn alloy via refinement and uniform dispersion of Mg₂Ca particles. *J Mater Sci Technol* 59:61–71. <https://doi.org/10.1016/j.jmst.2020.02.092>
- [19] Sun LX, Bai J, Xue F, Tao L, Chu CC, Meng J (2017) Exceptional texture evolution induced by multi-pass cold drawing of magnesium alloy. *Mater Des* 135:267–274. <https://doi.org/10.1016/j.matdes.2017.09.027>
- [20] Cai H, Zhang Y, Meng J, Li X, Xue F, Chu CL, Tao L, Bai J (2018) Enhanced fully-biodegradable Mg/PLA composite rod: effect of surface modification of Mg–2Zn wire on the interfacial bonding. *Surf Coat Technol* 350:722–731. <https://doi.org/10.1016/j.surfcoat.2018.07.045>
- [21] Cai H, Meng J, Li X, Xue F, Chu CL, Guo C, Bai J (2019) In vitro degradation behavior of Mg wire/poly(lactic acid) composite rods prepared by hot pressing and hot drawing.

- Acta Biomater 98:125–141. <https://doi.org/10.1016/j.actbio.2019.05.059>
- [22] Pitt HA, Nakeeb A, Espat NJ (2012) In: Jarnagin WR, Blumgart LH (eds) Blumgart's surgery of the liver, pancreas and biliary tract, 5th edn. Elsevier, Philadelphia, pp 113–122
- [23] Lu J, Wu DH, Rohani S (2014) Influence of Ca^{2+} on cholesterol crystallization from supersaturated model bile. Fluid Phase Equilib 367:51–56. <https://doi.org/10.1016/j.fluid.2014.01.031>
- [24] William H, Admirand SDM (1968) The physicochemical basis of cholesterol formation in man. J Clin Invest 47:1043–1052. <https://doi.org/10.1172/JCI105794>
- [25] Zhu YQ, Yang K, Cheng RY, Xiang Y, Yuan TW, Cheng YS, Sarment OB, Cui WG (2017) The current status of biodegradable stent to treat benign luminal disease. Mater Today 20:516–529. <https://doi.org/10.1016/j.mattod.2017.05.002>
- [26] Liu YH, Zhang PH (2016) Characterization of compression behaviors of fully covered biodegradable polydioxanone biliary stent for human body: a numerical approach by finite element model. J Mech Behav Biomed 62:128–138. <https://doi.org/10.1016/j.jmbbm.2016.04.029>
- [27] Zou QH, Xue W, Lin J, Fu YJ, Guan GP, Wang FJ, Wang L (2016) Mechanical characteristics of novel polyester/NiTi wires braided composite stent for the medical application. Results Phys 6:440–446. <https://doi.org/10.1016/j.rinp.2016.07.007>
- [28] Nicolas F, Renick DL, Ryo T, Juan LG, Alessio M (2014) Impact of stent strut design in metallic stents and biodegradable scaffolds. Int J Cardiol 177:800–808. <https://doi.org/10.1016/j.ijcard.2014.09.143>
- [29] Sanchez AHM, Luthringer BJC, Feyerabend F, Willumeit R (2015) Mg and Mg alloys: how comparable are in vitro and in vivo corrosion rates? A review. Acta Biomater 13:16–31. <https://doi.org/10.1016/j.actbio.2014.11.048>
- [30] Meng B, Wang J, Zhu N, Meng QY, Cui FZ, Xu YX (2006) Study of biodegradable and self-expandable PLLA helical biliary stent in vivo and in vitro. J Mater Sci Mater Med 17:611–617. <https://doi.org/10.1007/s10856-006-9223-9>
- [31] Zhao SJ, Liu XY, Gu LX (2012) The impact of wire stent fabrication technique on the performance of stent placement. J Med Devices 1:007–011. <https://doi.org/10.1115/1.4005788>
- [32] Yan TT, Tan LL, Xiong DS, Liu XJ, Zhang BC, Yang K (2010) Fluoride treatment and in vitro corrosion behavior of an AZ31B magnesium alloy. Mater Sci Eng C Mater 30:740–748. <https://doi.org/10.1016/j.msec.2010.03.007>
- [33] Preeti M, Jin KH, Andrew RP, Ihho P, Byoung-Gi M, Taek LB (2018) Development and properties of duplex MgF2/PCL coatings on biodegradable magnesium alloy for biomedical applications. PLoS ONE 13:e193927. <https://doi.org/10.1371/journal.pone.0193927>
- [34] Zeng RC, Cui LY, Jiang K, Liu R, Zhao BD, Zheng YF (2016) In vitro corrosion and cytocompatibility of a microarc oxidation coating and poly(L-lactic acid) composite coating on Mg–1Li–1Ca alloy for orthopedic implants. ACS Appl Mater Interfaces 8:10014–10028. <https://doi.org/10.1021/acami.6b00527>
- [35] Chen LX, Sheng YY, Zhou HY, Li ZB, Wang XJ, Li W (2019) Influence of a MAO + PLGA coating on biocorrosion and stress corrosion cracking behavior of a magnesium alloy in a physiological environment. Corros Sci 148:134–143. <https://doi.org/10.1016/j.corsci.2018.12.005>

Publisher's Note Springer Nature remains neutral with regard to jurisdictional claims in published maps and institutional affiliations.